17th World Conference on Earthquake Engineering, 17WCEE
Sendai, Japan - September 13th to 18th 2020

DESIGN AND CONTROL STRATEGIES FOR DYNAMICALLY SUBSTRUCTURED SYSTEMS (DSS)

V.P.Mehta[(1)], K. Muthumani[(2)]

[(1)] *Ph.D. student, Yokohama National University, Japan, mehta-vaibhav-rx@ynu.jp*
[(2)] *Professor, VIT University, India, muthumanik@yahoo.com*

Abstract

Dynamically substructured system (DSS) is a relatively new method which seeks to avoid these problems by performing tests on key elements of the structure at full or large scale, with the physical test coupled in real-time with the numerical model of the surrounding structure. In this on-going research, an effort has been made to understand the extensibility and capability of substructuring techniques to simulate structural behavior through different types of controllers specifically H_∞ (H-infinity), H_2 / H_∞ and linear–quadratic regulator (LQR) based controllers. The H_∞ part of the design guarantees the closed-loop stability for the unmodeled dynamics of the system and the H2 part deals with the issue of minimizing the energy of the system. The LQR algorithm reduces the amount of work done by the control systems engineer to optimize the controller. Control toolbox of MATLAB has been used for the design of the controllers and to achieve the desired control objective. Forced Based DSS of the steel framed structure is considered for the study. Linear time invariant (LTI) system with linear model for electromagnetic shaker is taken into consideration. As per the analytical results, it has been found that the controllers satisfy the desired control objective. The control law is validated by checking the impulse and step response of the system. The control objective is checked for its stability criterion as well. Nyquist plot refereed as the parametric plot showing the frequency response of the system also validates the control law showing that the system is controllable. The linearity justifying the finite dimension of the system is validated by the numerical result of the pole-zero map of the proposed DSS. The Open-loop phase and open-loop gain obtained from Nichols chart checks the robustness of the linear system. Bode plots of different controllers for the proposed DSS also shows a close agreement between the force transferred by the AMD and NS Also, limitations of the testing system are incorporated as the constraints in the optimization problem and the effect of such constraints of the control inputs on the DSS error have been investigated. It has been found that with increase in the weights on the control input (u), DSS error increases. H_2 / H_∞ controller can be of a good choice amongst the others if to minimize the energy is the criteria. However, the validation of the control strategy discussed in this paper will be experimentally validated in future work.

Keywords: Dynamic substructure; H_∞ **;** H_2 / H_∞ *; LQR; MATLAB*

1. INTRODUCTION

Recent advancements in earthquake engineering research have produced an array of experimental equipment and testing capabilities worldwide. It is often difficult to check the dynamic responses of the civil engineering structures to seismic loads with complete accuracy. Hence hybrid simulation technique was introduced in an attempt to quantify the damages occurred due to the earthquake and this technique was first proposed wherein the seismic response of a single-degree-of-freedom (SDOF) system was obtained with an analogue computer [1]. Laboratories are often equipped with shake tables, ranging from uni-axial tables to six-degree-of-freedom tables to multiple table arrays [2-7]. However, full-scale dynamic testing of civil engineering structures is extremely costly and difficult to perform. Most test methods, therefore, involves either a reduction in the physical scale or an extension of the timescale. Both approaches can cause significant difficulties in extrapolating to the full-scale dynamic behavior, particularly when the structure responds nonlinearly or includes highly rate-dependent components such as dampers [9]. Innovative advances in the field of substructuring techniques gave rise to an extremely new concept of distributed pseudo dynamic testing generally coined as geographically-distributed testing but however this technique has its own limitations. It is often difficult to check the dynamic responses of the civil engineering structures to seismic loads with complete accuracy. Dynamic substructure system (DSS) is a relatively new method [10-11] which seeks to avoid these problems by performing tests on key elements of the structure at full or large scale, with the physical test coupled in real-time with the numerical model of the surrounding structure. Nowadays, dynamic analysis of complex structures can be efficiently computed utilizing different available software [12-15]. The cost of computation has been ceaselessly lessened and now very complicated and detailed numerical simulations are conceivable on personal computers. Hence hybrid simulation technique incorporated with the DSS was introduced to quantify the damages occurred due to the earthquake [16-20]. DSS also called as real-time hybrid simulation and model-in-the-loop testing, is a technique used for response evaluation of complex structures. The structure under consideration, referred to as the emulated system [21], is divided into two parts—(a) a physical substructure (PS), which comprises the part of structure that is physically tested and (b) a numerical substructure (NS), which is a computational model of the remainder of the structure[22]

The essentiality in selecting this topic is to understand the concept of dynamic substructuring technique for evaluating the structural response to the dynamic loads. Moreover, for obvious economic reasons, full scale structures are rarely tested to destruction intentionally. The motivation for the present research is to extend dynamic substructuring techniques, with the hopes that hybrid simulation will continue to be an effective method of structural testing. Under this objective, the architecture of the hybrid simulations incorporated with the control theory has been studied in a broader perspective. The real challenge of DSS is to compensate for the dynamics of the transfer system (TS) and the sensors, and for the control–structure interaction, so that the resulting feedback system is stable, and the effect of the NS is represented sufficiently accurately. Other kinds of errors can also creep in, such as computational and measurement errors, and the performance of the substructuring must be robust to such errors. Hence based on these studies, different types of controllers specifically H_∞ (H-infinity), H_2 / H_∞ and linear–quadratic regulator (LQR) have been designed and investigated numerically in this paper to understand the robustness and effect of different types of controllers on DSS. The control design methodology is implemented to optimize the controllers for DSS. The designed controller for DSS are validated by various stablity criterion. Forced based DSS of a two-degree-of-freedom (2DOF) steel framed structure is considered for the study.The scope of the current research is limited to linear time-invariant (LTI) system with linear model of active mass driver (AMD)

2. MODELING OF THE SYSTEM

The heart of the DSS method is the separation of the structure in two or more parts. One part, the physical substructure (PS) which is tested on the loading frame and the other part, the numerical substructure (NS) which is a numerical model of the remainder of the structure. The boundary condition between the two substructures is applied with the help of a transfer system (TS). Two-storey shear building is adopted as the system whose response is emulated using hybrid simulation. The bottom storey is taken as the physical subsystem while the top storey is taken as the numerical subsystem. A control law is derived such that the mechanical impedance of the electromagnetic shaker matches to that of the virtual subsystem. The control law is validated by comparing the frequency responses of the virtual subsystem and the electromagnetic shaker from the physical subsystem acceleration to the force transferred

The full structure whose dynamic response needs to be 2DOF steel framed system is selected as emulated system as shown in Fig. 1a. Electromagnetic shaker is used as an active mass driver (AMD) to apply the boundary condition between the two substructures. The schematics of the hybrid system are shown in Fig. 1b. The mechanical properties of the numerical substructure (NS), physical substructure (PS) and AMD are given in the Table 1, where, m_{ns},m_{ps}, m_a,k_{ns}, k_{ps},k_a,c_{ns}, c_{ns}, c_a are the mass, stiffness and damping of the NS, PS and AMD respectively, G_v is the amplifier gain in voltage, Bl is the force per unit current.

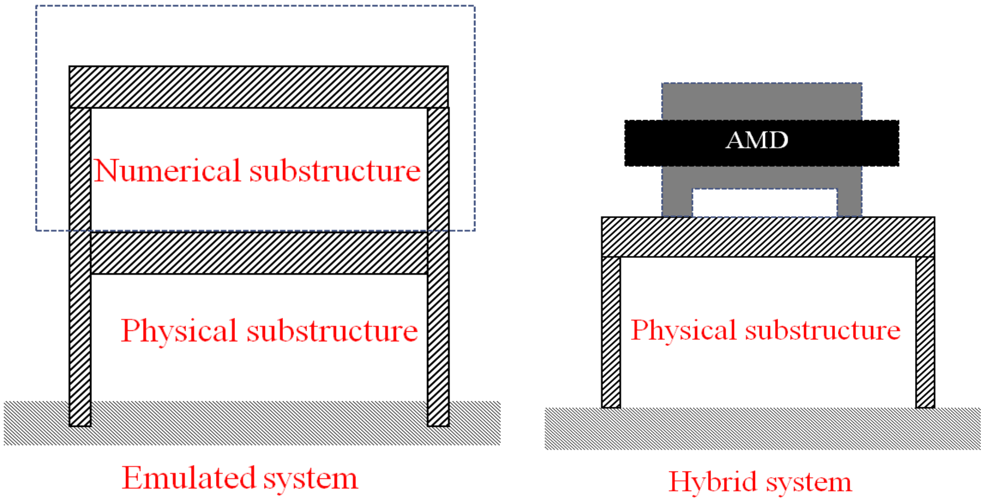

Fig. 1 (a) Emulated system (b) Schematics of hybrid system

Table 1 - The mechanical properties of the NS, PS and AMD

NS	PS	AMD	
m_{ns} = 17.9 kg	m_{ps}= 94 kg	m_a	17.9 kg
k_{ns}= 3 × 10^4 N/m	k_{ps}= 3× 10^5 N/m	c_a	25
c_{ns} = 42	c_{ns}= 106	k_a	175 N/m
		R	1.5
		G_v	-4
		L	.022m
		Bl	19.62 N/A

2.1 CONTROL DESIGN METHODOLOGY

The usual objective of control theory is to control a system, often called the plant, so its output follows a desired control signal, called the reference, which may be a fixed or changing value. To do this a controller is designed, which monitors the output and compares it with the reference. Control systems are an integral part of the DSS and are designed for controlling the errors in the transfer of forces in the NS and AMD. The interface condition between the two substructures is imposed on the PS, and the corresponding work conjugate is measured and fed back to the VS. The boundary conditions at the interface of the two substructures are intrinsic. However, in DS, it is implemented by means of a transfer system. The force transfer mechanism helps to understand the transfer of the force from the PS to AMD and vice-versa. It is essential to understand this mechanism as it plays a very significant role in the design of the controllers to be used for the DSS. The control objective is formulated as stated in Eq. (1). The control design procedure is illustrated with specific reference to an electromagnetic shaker used to imitate the NS. Although the methodology presented here is applicable more generally, for the sake of specificity, the configuration used in Fig. 2 is used as the basis for further discussion. Importantly, to demonstrate the effectiveness of the approach, a very lightly damped PS is chosen as reflected in table 1 as well, which poses major stability issues with the conventional approach. Fig. 2 (a) shows the configuration and the force transfer mechanism of the DSS used in the present study.

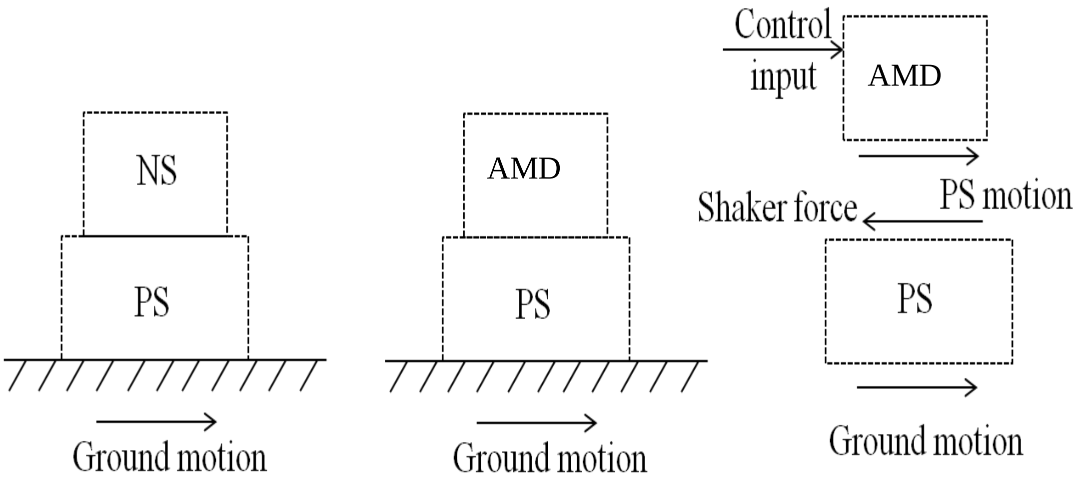

Fig.2 Dynamic substructuring configuration used in this research

Control Objective: - $f^{ns} = f^{AMD}$ (1)

Using the control literatures [23], the subsystem enclosed by a box in Fig 3 is termed as "augmented plant." The dynamics of the NS are represented in state-space form as (see Eq. 2,3 and 4)

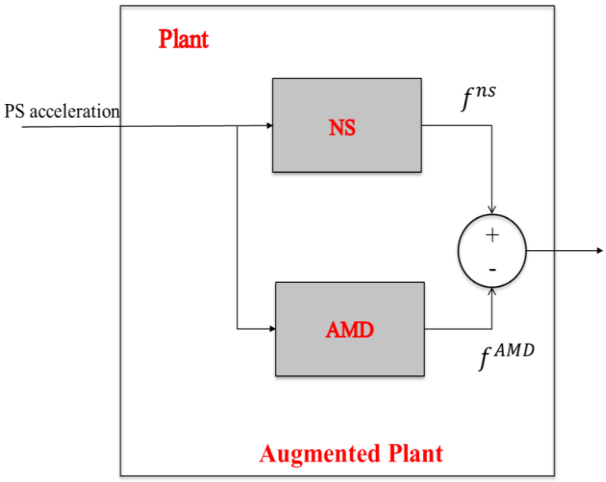

Fig.3. Conceptual representation of the augmented plant

3. MATHEMATICAL MODELLING OF DSS

This section illustrates the mathematical modelling of the physical system of DSS using state-space representation. The linear time invariant model of the system is taken into consideration with the AMD as linear model.

3.1 STATE-SPACE REPRESENTATION OF NS

The state-space equation of the NS is obtained from the dynamic equation of motion of SDOF system subjected to single support excitation. The equation of motion for SDOF system with single support excitations given by Eq. (2), Eq. (3) and Eq. (4)

$$m_{ns}\dot{x}_2 + k_{ns}x_1 + c_{ns}x_2 = -m_{ns}w \quad (2)$$

$$\begin{Bmatrix}\dot{x}_1\\ \dot{x}_2\end{Bmatrix} = \begin{bmatrix}0 & 1\\ \frac{-k_{ns}}{m_{ns}} & \frac{-c_{ns}}{m_{ns}}\end{bmatrix}\begin{Bmatrix}x_1\\ x_2\end{Bmatrix} + \begin{Bmatrix}0\\ -1\end{Bmatrix}w \quad (3)$$

$$z = [k_{ns} \;\; c_{ns}]\begin{Bmatrix}x_1\\ x_2\end{Bmatrix} \quad (4)$$

where, $x_1 = x$ *i*.e. displacement of the NS $x_2 = v$ i.e. velocity of the NS, w= ground acceleration $\dot{x}_2$= acceleration of the system

3.2 STATE-SPACE REPRESENTATION OF AMD

The active mass driver AMD or the electromagnetic shaker as it is often called, is significant in the control modelling of DSS. The electromagnetic shaker has a high frequency bandwidth, low distortion, and linear behavior. These shakers have been widely used for critical equipment qualification in aerospace and automotive industries [24,25]. Interestingly, the dynamics of electromagnetic and hydraulic shakers are remarkably similar [26]. The natural velocity feedback [27] in hydraulic shaker is akin to back electromotive force (EMF) in electromagnetic shaker. The linearized model of the hydraulic shaker has three poles (and few additional poles if servo valve dynamics are also modeled) and so does the electromagnetic shaker model. Due to the similar nature of the two shakers, the conclusions from the experiments are meaningful for hydraulic actuators as well.
The model discussed here is based on Lang [28] In an AMD, a coil of wire (armature) is suspended in a uniform magnetic field, B (see Figure 4). An axial force is produced by current, passing through the suspended coil. The magnitude of the force is proportional to the instantaneous value of the current and acts in the direction mutually perpendicular to the directions of the current and the magnetic field. Hence, the force experienced by the armature is equal to Blx_3 where l is the length of the conductor making up the coil. The motion of the armature is resisted by the restoring force due to the stiffness of suspension bands, k_a, built in the shaker for recentering, and the overall damping is c_a. The overall damping accounts for both inherent mechanical and eddy current damping. The equation of motion of the armature can be written as given in Eq. (5)

$$m_a\dot{x}_2 + k_a x_1 + c_a x_2 = Blx_3 - m_a w \quad (5)$$

where m_a is the moving mass of the armature, represent the displacement and velocity of armature assembly, respectively, and w is the acceleration input at the base of the shaker (eventually, the PS acceleration). The motion of the armature in turn produces back EMF E_b= $-Blx_2$, which opposes the externally applied voltage (equal to amplifier gain, Gv, times voltage input u). The current is related to the externally applied voltage by Kirchoff's voltage law and is given by Eq. (6)

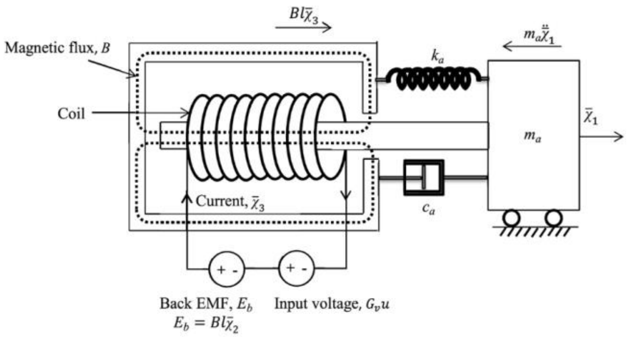

Fig. 4. Schematic of active mass driver (AMD)

$$G_v u - Blx_2 = Rx_3 + L\dot{x_3} \tag{6}$$

where R and L are the resistance and inductance of the armature coil, respectively. For the AMD, the system is represented by a collection of the coupled linear first-order differential equation and using Eq. (5) and Eq. (6) The state-space equations are assembled in the form of the matrix as shown in Eq. (7, 8) where, x_1 is the displacement of the PS, x_2 is the velocity of the PS, x_3 is the current of the PS, $\dot{x_2}$ is acceleration of the PS and w is the ground acceleration as mentioned in the earlier section.

$$\begin{Bmatrix}\dot{x}_1\\ \dot{x}_2\\ \dot{x}_3\end{Bmatrix} = \begin{bmatrix} 0 & 1 & 0 \\ \frac{-k_a}{m_a} & -\frac{c_a}{m_a} & \frac{Bl}{m_a} \\ 0 & \frac{-B\,l}{L} & \frac{-R}{L} \end{bmatrix} + \begin{Bmatrix}x_1\\ x_2\\ x_3\end{Bmatrix} + \begin{Bmatrix}0\\ 0\\ \frac{G_v}{L}\end{Bmatrix} u + \begin{Bmatrix}0\\ -1\\ 0\end{Bmatrix} w \tag{7}$$

$$\mathrm{z} = \begin{bmatrix}0 & 0 & -Bl\end{bmatrix} \begin{Bmatrix}x_1\\ x_2\\ x_3\end{Bmatrix} \tag{8}$$

3.3 STATE-SPACE REPRESENTATION OF AUGMENTED PLANT

Augmented plant is the combined plant containing the combined matrices of the NS and AMD assembled together. The following matrix shows the state-space equations for the augmented plant as given in Eq. (9)

$$\begin{Bmatrix}\dot{x}_1\\ \dot{x}_2\\ \dot{x}_3\\ \dot{x}_4\\ \dot{x}_5\end{Bmatrix} = \begin{bmatrix} 0 & 1 & 0 & 0 & 0 \\ \frac{-k_{ns}}{m_{ns}} & -\frac{c_{ns}}{m_{ns}} & 0 & 0 & 0 \\ 0 & 0 & 0 & 1 & 0 \\ 0 & 0 & \frac{-k_a}{m_a} & -\frac{c_a}{m_a} & \frac{B\,l}{m_a} \\ 0 & 0 & 0 & \frac{-B\,l}{L} & \frac{-R}{L} \end{bmatrix} \begin{Bmatrix}x_1\\ x_2\\ x_3\\ x_4\\ x_5\end{Bmatrix} + \begin{Bmatrix}0\\ 0\\ 0\\ 0\\ \frac{\mathrm{G_v}}{\mathrm{L}}\end{Bmatrix} u + \begin{Bmatrix}0\\ -1\\ 0\\ -1\\ 0\end{Bmatrix} w \tag{9}$$

4. DESCRIPTION OF CONTROLLER DESIGN

This section describes the various controller design methodology used for the DSS proposed in this paper namely H_∞ , H_2 / H_∞ and LQR type of controllers

4.7 DESIGN OF H_∞ AND H_2 / H_∞ CONTROLLER DESIGN

H_∞ methods are used in control theory to synthesize controllers achieving stabilization with guaranteed performance. Robust Control Toolbox of MATLAB commands are used to apply the powerful methods of H_∞ synthesis to control design problems for achieving the desired control objective. To use H_∞ methods, the control problem is expressed as a mathematical optimization H_∞ techniques have the advantage over classical control techniques in that they are readily applicable to problems involving multivariate systems with cross-coupling between channels; disadvantages of H_∞ techniques include the level of mathematical understanding needed to apply them successfully and the need for a reasonably good model of the system to be controlled. It is important to keep in mind that the resulting controller is only optimal with respect to the prescribed cost function and does not necessarily represent the best controller in terms of the usual performance measures used to evaluate controllers such as settling time, energy expended, etc.

4.7.1 Problem formulation

The plant *P* has two inputs, the exogenous input *w*, that includes reference signal and disturbances, and the manipulated variables *u*. There are two outputs, the error signals *z* that we want to minimize, and the measured variables *v*, that we use to control the system. *v* is used in *K* to calculate the manipulated variable *u*. Notice that all these are generally vectors whereas P and K are matrices. First, the process must be represented according to the following standard configuration as shown in fig. 5. The H_∞ part of the design gurantees the closed-loop stability for the unmodeled dynamics of the system and the H_2 part deals with the issue of minimizing the energy of the system. In order to overcome the limitations of H-infinity based method of controller design, H_2 / H_∞ based method of controller design is used to improve the robustness of the controller thus obtained. The standard configuration of H_2 / H_∞ based controller **is** shown in fig. 5 by which the desired controller is designed and evaluated for achieving the control objective. Control Toolbox of MATLAB is used for the controller design. The plant must be stabilizable from the control inputs *u* and detectable from the measurement output *y*.

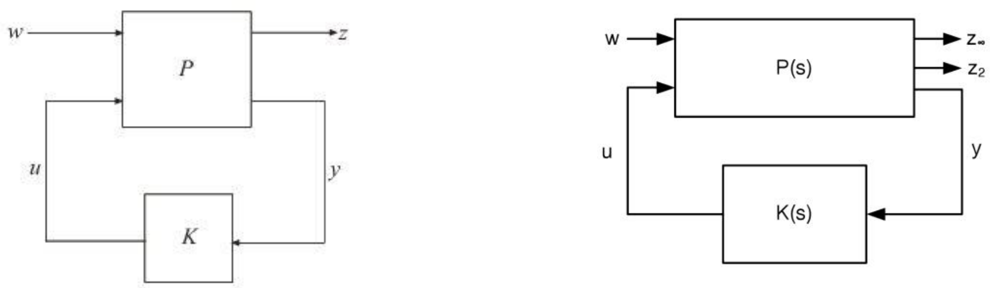

Fig.5. Standard configuration for H_∞ and H_2 / H_∞ controller (MATLAB Control Toolbox)

4.9 DESIGN OF LQR CONTROLLER DESIGN

The settings of a controller governing either a machine or process are found by using a mathematical algorithm that minimizes the cost function with weighting factors supplied by an engineer. The cost function is often defined as a sum of the deviations of key measurements, desired altitude or process temperature, from their desired values. The algorithm thus finds those controller settings that minimize undesired deviations. The magnitude of the control action itself may also be included in the cost function. The theory of optimal control is concerned with operating a dynamic system at minimum cost. The case where the system dynamics are described by a set oflinear differential equations and the cost is described by a quadratic is called the LQ problem. One of the main results in the theory is that the solution is provided by the linear–quadratic regulator (LQR).

The LQR algorithm reduces the amount of work done by the control systems engineer to optimize the controller. However, the engineer still needs to specify the cost function parameters, and compare the results with the specified design goals. Often this means that controller construction will be an iterative process in which the engineer judges the "optimal" controllers produced through simulation and then adjusts the parameters to produce a controller more consistent with design goals. Control Toolbox of MATLAB is used for the controller design. For a continuous time, system, the state-feedback law $u = -Kx$ minimizes the quadratic cost function subject to the system dynamics given by the state-space equations.
The finite horizon, linear quadratic regulator (LQR) is given by

$$J(u) = \int_0^{\infty} (x^T Q x + u^T R u + 2x^T N u) dt \tag{10}$$

Where Q and R are the positive definite matrices.

5. VALIDATION FOR STABILITY CRITERIORN

Fig 6 shows the step and impulse response of the DSS. It is seen that the time behaviour of the output of the system changes from zero to one in a very short time. It indicates that the overshooting time is less than a second followed by the ringing and all subsiding within the settling time and henceforth the system is stable. The step response of the system confirms its stability criterion. Formally, knowing the step response of a dynamical system gives information on the stability of such a system, and on its ability to reach one stationary state when starting from another.

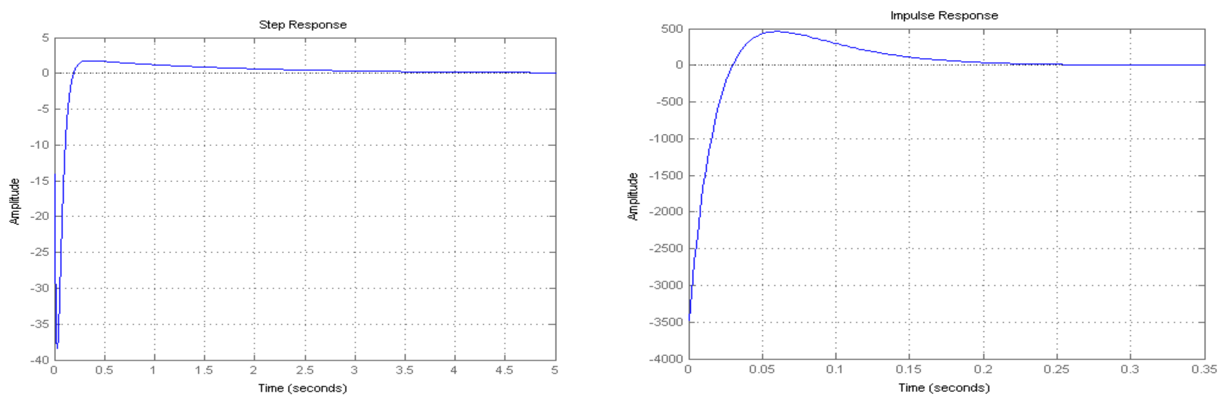

Fig. 6. Step and Impulse response of the DSS

From the impulse response function in the fig. 6 it is seen that the impulse response decays slower. The impulse response strongly depends on the damping and which thereby impacts the root-mean-square (rms) value of the response. For small damping the rms response of the system is larger than that of the larger damping. The pole-zero map of the DSS is shown in fig. 7. The poles are complex with small real parts and are non-clustered indicating the linearity of the system and justifying the finite dimension of the system. Its distance from the origin is the natural frequency of the structure. shows Root locus graph and Nyquist plot for the DSS Open-loop phase and open-loop gain are obtained which is used for checking the robustness of the linear system incorporated for the DSS. Hence, the system is robust is nature. Nyquist plot is a parametric plot showing the frequency response of the system and thereby showing that the system is controllable. The angle at which the curve approaches origin gives the shape and depth of the transfer function. The control law is validated by checking the impulse and step response of the system. The control objective is checked for its stability criterion as well. Nyquist plot refereed as the parametric plot showing the frequency response of the system also validates the control law showing that the system is controllable. The linearity justifying the finite dimension of the system is validated by the numerical result of the pole-zero map of the proposed DSS

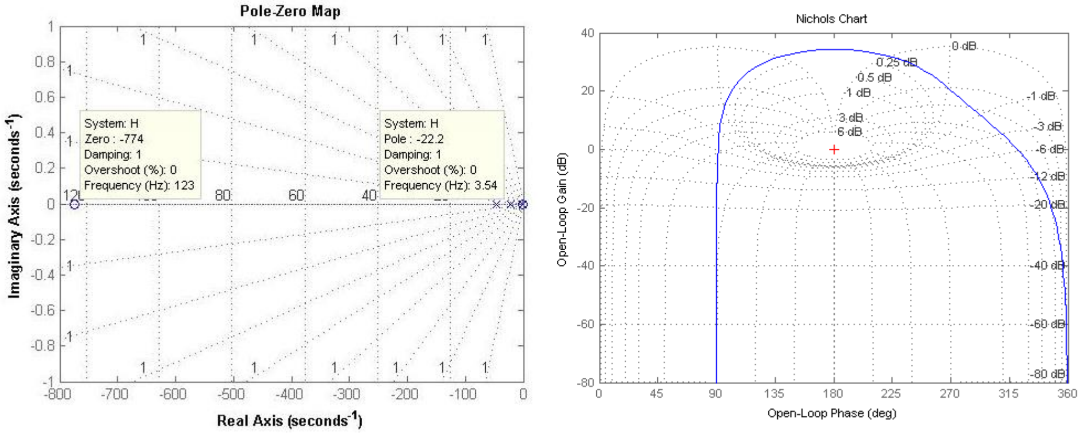

Fig. 7. Pole-Zero map and Nichols chart for the DSS

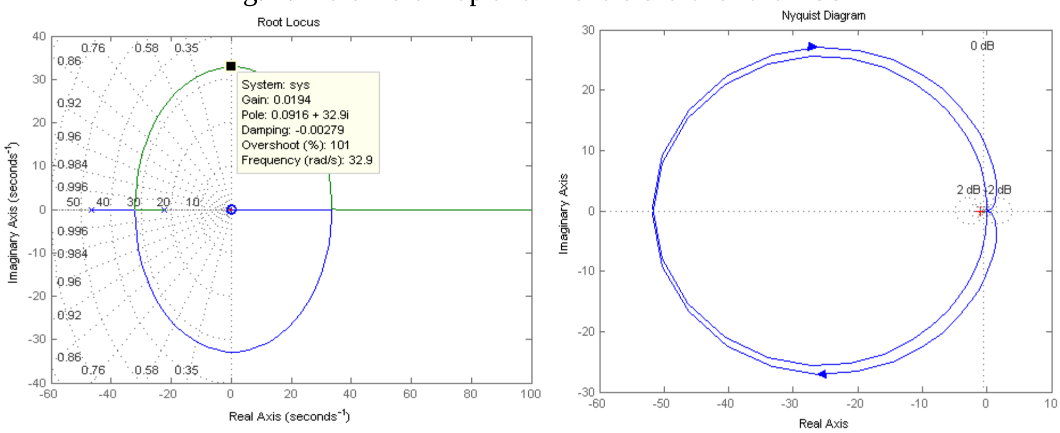

Fig. 8. Root locus graph and Nyquist plot for the DSS

6.2 VALIDATION OF THE CONTROLLERS FOR THE DESIRED CONTROL OBJECTIVE

Fig.8 shows the bode plot for the H_∞ controller and it shows a close agreement between the force transferred by the AMD and NS. This shows that the designed controller can be used for controlling the force transfer. The graphical representation of the variation of DSS error vs weights on control is shown in fig. 9. This graph shows that the DSS error can be kept minimum by keeping the weight on the constraints in the range of 10-100, however with the increase in the weight on the constraints of the control input, the DSS error also increases. Therefore, within the specified range a good match of force transferred by NS and AMD is obtained.

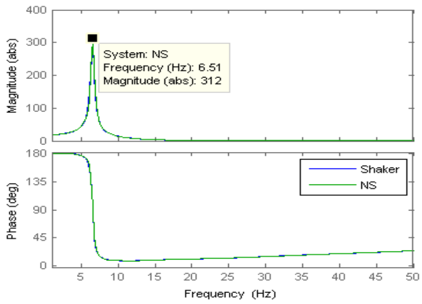

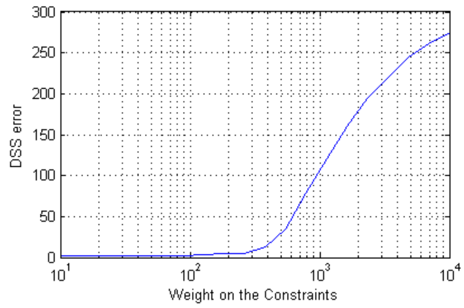

Fig.8 . Bode plot for H∞ controller and Fig.9 . Graphical representation of the variation of DSS error vs weights on control

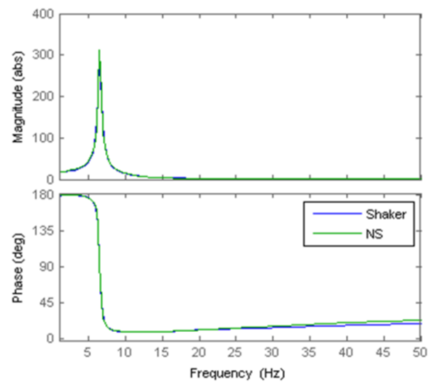

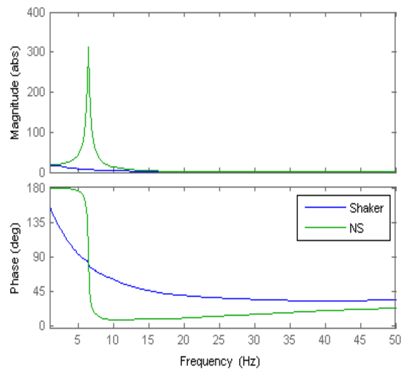

Fig.10. Bode plot for LQR controller and Fig11. Bode plot for LQR controller with increased weight on the control input

LQR controller gives a good match between the force transferred by the NS and AMD. A phase transfer of 180 degrees can be seen at the resonating frequencies in fig. 10. However, if we increase the weight on the control input of the LQR controller, the control objective is not satisfied and is shown in fig. 11.

6. CONCLUSIONS

The DSS technique has been shown to work for a wide range of controllers. As per the analytical results, it has been found that all the controllers satisfy the desired control objective. The control law is validated by checking the impulse and step response of the system. The control objective is checked for its stability criterion as well. Nyquist plot refereed as the parametric plot showing the frequency response of the system also validates the control law showing that the system is controllable. The linearity justifying the finite dimension of the system is validated by the numerical result of the pole-zero map of the proposed DSS. The Open-loop phase and open-loop gain obtained from Nichols chart checks the robustness of the linear system. Bode plots of different controllers for the proposed DSS also shows a close agreement between the force transferred by the AMD and NS Also, limitations of the testing system are incorporated as the constraints in the optimization problem and the effect of such constraints of the control inputs on the DSS error have been investigated. It has been found that with increase in the weights on the control input (u), DSS error increases. H_2/ H_∞ controller can be of a good choice amongst the others if to minimize the energy is the criteria. However, the validation of the control strategy discussed in this paper will be experimentally validated in future work.

7. REFERENCES

[1] Hakuno, M., Shidawara, M., & Hara, T. (1969): Dynamic destructive test of a cantilever beam controlled by an analog-computer *Trans. Jpn Soc. Civ. Engrs,* 171: 1-9.

[2]Takahashi, Y., Nakashima, M., (1987), Japanese activities on online testing. *Journal of Engineering Mechanics*, *ASEC*. Vol. 113, pp. 1014-1032.

[3] Brownjohn J.M.W., Dumanoglu A. A., Severn R. T. and Taylor C. A. (1987): Ambient vibration measurements of the humber suspension bridge and comparison with calculated characteristics. *Proc. Inst. Civ. Engrs.* Vol . 83, pp. 561-600.

[4] Reinhorn, A.M., Soong, T.T., Riley, M.A., Lin, R.C., Aizawa, S., Higashino, M. (1993):Full Scale implementation of active control Part II: Installation and performance. *Journal of Structural Engineering, ASCE* Vol. 119, No. 6, pp. 1938-1960.

[5]Takanashi, K. et al . (1974):Seismic failure analysis of structures by computer-pulsator on-line system.*J. Inst, of Industrial Sci.,* Univ. o f Tokyo, Tokio, Japan, 26(11): 13-25. (In Japanese).

[6]Takanashi, K., & Ohi, K. (1983):Earthquake response analysis of steel structures by rapid computer-actuator on-line system, (1) a progress report, trial system and dynamic response o f steel beams. *Bull. Earthquake Resistant Struct. Research Center (ERS*), Inst, of Industrial Sci., Univ. of Tokyo, Tokyo, Japan, 16: 103-109.

[7]Takanashi, K., Udagawa, K., & Tanaka, H. (1978): Earthquake response analysis of steel frames by computer-actuator on-line system". *Proc., 5th Japan Earthquake Engrg.Symp.,* 1321-1328.

[8]Takanashi, K., Udagawa, K., Seki, M., Okada, T., & Tanaka H. (1975):Nonlinear earthquake response analysis o f structures by a computer-actuator on-line system*Bulletin o f Earthquake Resistant Structure Research*

[9]Blakeborough, A., Williams, M. S., Darby, A. P., & Williams, D. M. (2001):The development of real-time substructure testing.*Philosophical Transaction o f the Royal Society: Theme Issue on Dynamic Testing of Structures,* A 359: 1869-1891.

[10] Goldman, R. L. (1969): Vibration analysis by dynamic partitioning. *AIAA journal*, *7*(6), 1152-1154

[11] Reinhorn, A. M., Sivaselvan, M. V., Liang, Z., Shao, X., Pitman, M., & Weinreber, S. (2005):Large scale real time dynamic hybrid testing technique-shake tables substructure testing. In *Proc. Int. Conf. Adv. Exp. Struct. Eng* (Vol. 1, pp. 457-464).

[12] Rubin, S. (1975): Improved component-mode representation for structural dynamic analysis. *AIAA journal*, *13*(8), 995-1006.

[13]Darby, A. P., Blakeborough, A., & Williams, M. S. (1999):Real-time substructure tests using hydraulic actuator.*Journal of Engineering Mechanics,* ASCE, 125(10): 1133- 1139.

[14] Bouhaddi, N., & Fillod, R. (1996):Substructuring by a two level dynamic condensation method. *Computers & structures*, *60*(3), 403-409.

[15] Verma, M., Rajasankar, J., & Iyer, N. R. (2014). Fuzzy logic controller for real-time substructuring applications. *Journal of Vibration and Control*, *20*(8), 1103-1118..

[16]Horiuchi, T., Inoue, M., Konno, T., & Namita Y. (1999):Real-time hybrid experimental system with actuator delay compensation and its application to a piping system with energy absorber.*Earthquake Engineering and Structural Dynamics,* 28(10): 1121-1141.

[17]Horiuchi, T., Inoue, M., Konno, T., & Namita Y. (1999):Real-time hybrid experimental system with actuator delay compensation and its application to a piping system with energy absorber.*Earthquake Engineering and Structural Dynamics,* 28(10): 1121-1141.

[18] Horiuchi, T., Nakagawa, M., Sugano, M., & Konno, T. (1996):Development of a realtime hybrid experimental system with actuator delay compensation.*In Proc. 11th World Conf. Earthquake Engineering*, Paper No. 660.

[19]Dermitzakis, S. N., & Mahin, S. A. (1985):Development of substructuring techniques for on-line computer controlled seismic performance testing.*Report UCB/EERC-85/04,* Earthquake Engineering Research Center, University o f California, Berkeley.

[20]Nakashima, M., & Masaoka, N. (1999):Real time on-line test for MDOF systems.*Earthquake Engineering and Structural Dynamics,* 28(4):393-420.

[21] Wallace, M. I., Sieber, J., Neild, S. A., Wagg, D. J., & Krauskopf, B. (2005):Stability analysis of real-time dynamic substructuring using delay differential equation models. *Earthquake engineering & structural dynamics*, *34*(15), 1817-1832.

[22] Verma, M., Sivaselvan, M. V., & Rajasankar, J. (2019):Real-time Hybrid Simulation Using an Electromagnetic Shaker. In *Recent Advances in Structural Engineering, Volume 2* (pp. 119-128). Springer, Singapore.

[23] Boyd, S., El Ghaoui, L., Feron, E., & Balakrishnan, V. (1994):Linear matrix inequalities in system and control theory (Vol. 15). Siam.

[24] McCrum, D. P., & Williams, M. S. (2016): An overview of seismic hybrid testing of engineering structures. Engineering Structures, 118, 240-261.

[25] Wang, M. L., Shah, S. P., & Baker, J. P. (1990): An electromagnetic closed-loop materials testing station. *Experimental Techniques*, *14*(4), 52-55

[26] Dyke, S. J., Spencer Jr, B. F., Quast, P., & Sain, M. K. (1995): Role of control-structure interaction in protective system design. *Journal of Engineering Mechanics*, *121*(2), 322-338.

[27] Carl, J., & Sivaselvan, M. V. (2011): Improved dynamic testing by impedance control. *Earthquake Engineering and Engineering Vibration*, *10*(3), 423.

[28] Lang, G. F. (1997): Electrodynamic shaker fundamentals. *Sound and vibration*, *31*(4), 14-23.

